Wireless Personal Communications (2005) 33: 87–108
DOI: 10.1007/s11277-005-7224-5

The Impact of Estimation Error and Dwell Time on the Performance of Predetection Selection Diversity Receivers

SÉBASTIEN ROY and JEAN-SÉBASTIEN NÉRON

Département de génie électrique et de génie informatique, Université Laval, Québec, QC, Canada, G1K 7P4
E-mail: sebasroy@gel.ulaval.ca

Abstract. Selection diversity is a simple and potentially cost-effective combining method to combat fading with an antenna array. However, it is often assumed for true selection diversity (SD) and some of its variants that all branches are available all the time, i.e., that the receiver chain is duplicated for all elements. This allows the selection step to be performed after signal detection. Yet, since only one branch is used in SD at any given time to receive the desired signal, this diversity scheme can be implemented with a single complete receiver chain, switching means, and some simple means to measure signal power in each branch. This paper explores related practical issues, including the incorporation of the proposed scheme in 802.11-based wireless LANs and GSM cellular networks, and provides a performance analysis for such a selection diversity combiner implemented with inexpensive Schottky diodes as signal power measurement devices. Since power measurements thus obtained are noisy, the impact on performance is assessed through analysis in Rayleigh-fading environments. Performance parameters (PDF of output SNR, average output SNR, bit error probability for any modulation scheme) are obtained in closed-form and are compared with ideal selection diversity. It is found that performance can easily be less than 0.5 dB away from ideal selection diversity. Furthermore, the analysis is extended to include the effect of prolonged dwell time, i.e., the minimum interval between switching cycles is longer than the channel coherence time.

Keywords: antenna arrays, array signal processing, diversity combining, selection diversity

1. Introduction

Selection diversity combining (SDC) constitutes a very simple and cost-effective strategy to exploit an antenna array (or any other diversity source, such as the multiple rays in a RAKE-type receiver) to combat multipath fading. In principle, a selection diversity combiner works by selecting at all times the branch with the highest signal-to-noise ratio (SNR) for signal reception. Hence, it requires only a single receiver chain (downconverter, demodulator, sampler, detector, etc.) provided that adequate switching means are present.

Classical theoretical results on selection diversity assume (1) that SNR measurements are noise-free and (2) that based on these measurements, the switch to the best branch is instantaneous. While this is obviously analytically convenient and useful for many purposes – including comparing diversity strategies – it does not yield a realistic performance assessment. Indeed, it is difficult in practice to extract *only* the desired signal power and some degree of noise invariably remains.

It is noteworthy that some authors have looked at the impact of switching constraints [1, 2] which include physical switching delays and system-imposed dwell times (to avoid information loss during switching). Both papers examine the performance degradation in selection diversity when a given branch selection must be maintained for a certain amount of

time while the channels are changing. In both cases, it was found that a significant degradation is observed when the dwell time reaches 10% of the channel decorrelation time.

1.1. SDC WITH A SINGLE RECEIVER CHAIN

There seems to be a common assumption in the literature that SDC necessarily implies that full receiver chains are present on all branches. In fact, it is often assumed that the availability of a single receiver chain implies a simpler threshold-based "switched" diversity strategy (such as "switch-and-stay" and "switch-and-examine") [3–5] which brings about a significant performance loss since these do not even attempt to select the best branch. The following discussion provides an overview of the topic and a motivation for the implementation of true SDC based on a single receiver chain.

It was recognized in [6] that typical power measurement devices in practical selection combiners would yield signal-plus-noise (S + N) power instead of signal-to-noise ratio. The performance analysis therein shows that combiners based on signal-plus-noise measurements perform *better* than combiners based on the signal-to-noise ratio measure. However, this assumes that (1) the system has full receiver chains on each branch, (2) it is capable of picking the best branch on a symbol-by-symbol basis and (3) it selects the said branch based on S+N measurements for *the symbol to be detected*. Hence, a branch has more chance of being selected when the noise sample adds up constructively with the useful signal. However, and while such a strategy may sometimes make sense (since it is numerically simpler than maximal ratio combining for example), it is impossible to implement with a single receiver chain and in that sense defeats the purpose of using selection diversity.

In the same vein, improved selection diversity strategies based on branch log-likelihood ratios and yielding even superior performance were presented in [8]. Such strategies, which rely on the availability of demodulated data on all branches to improve the performance of classical SDC, have collectively become known as *postdetection selection combining* [6, 8–10]. A similar approach was proposed for switched diversity under the name *postdetection switched diversity*; this was thoroughly analyzed in [11, 12].

While these postdetection schemes display interesting performance improvements and certainly have their place, they are not in general cost-effective SDC implementations from an RF hardware point-of-view. Indeed, the cost of a receiver will almost always be dominated by the RF portion. Current digital signal processing capability is very affordable, and its price is continuously decreasing according to Moore's law. RF circuitry, on the other hand, is still relatively expensive and does not generally follow a trend similar to Moore's law. In light of this, a cost-effective implementation of selection diversity should be limited to a single receiver chain. If full receiver duplication is used, then a move to a more evolved diversity scheme (such as equal-gain combining or maximal ratio combining) is warranted, since the added numerical complexity will in most cases not increase system cost significantly.

1.2. PAPER OUTLINE

Given the above practical motivations for restricting selection diversity to a single receiver branch, this paper examines relevant practical receiver architectures. Unlike threshold-based switched-diversity schemes, SDC requires a means to estimate signal power in all branches, not just on the currently active one. This is accomplished herein via the use of Schottky-diode-based

envelope detectors to measure signal-plus-noise power in each branch. While this is a very low-cost device, it is an effective estimation mechanism in a white noise, i.e., interference-free, environment. In the same spirit, low-cost PIN diodes can be employed as switching means to select the appropriate branch to pass on to a single receiver chain. Section 2 presents the proposed hardware architecture, discusses various trade-offs and alternatives, and shows how such receivers could be incorporated in wireless LANs complying with the 802.11 standard. Section 3 presents the performance analysis which includes the impact of noisy power measures, Section 4 extends the analysis to include the impact of prolonged selection dwell time, and Section 5 presents some numerical results in uncorrelated Rayleigh fading. Throughout the paper, SDC1 refers to ideal selection diversity and SDC2 to the proposed architectures.

2. Receiver Architecture

To take full advantage of the simplicity inherent to selection diversity, the receiver circuit should consist of three elements: (1) a single receiver chain, (2) switching means and (3) simple power measurement devices. Since only element (3) and its associated circuitry needs to be replicated in each branch, it is quite cost-sensitive. Therefore, only very inexpensive components (e.g., Schottky diodes, directional couplers, low-noise amplifiers (LNAs), etc.) are used. Likewise, the switching means can be constructed out of inexpensive PIN diodes. It follows that the cost of the receiver is relatively insensitive to the number of branches.

2.1. Circuit Description

A block diagram of the proposed RF front-end is shown in Figure 1. Directional couplers are used at the outputs of the LNAs in each branch to divert a tiny fraction of the incident power to envelope detectors for the purpose of monitoring the total signal power. Based on these power measurements, branch selection can be performed via a single pole multiple throw (SPMT) switch. For low-cost and other practical considerations, it makes sense to construct such switches out of PIN (positive-insulator-negative) diodes which are characterized by their fast

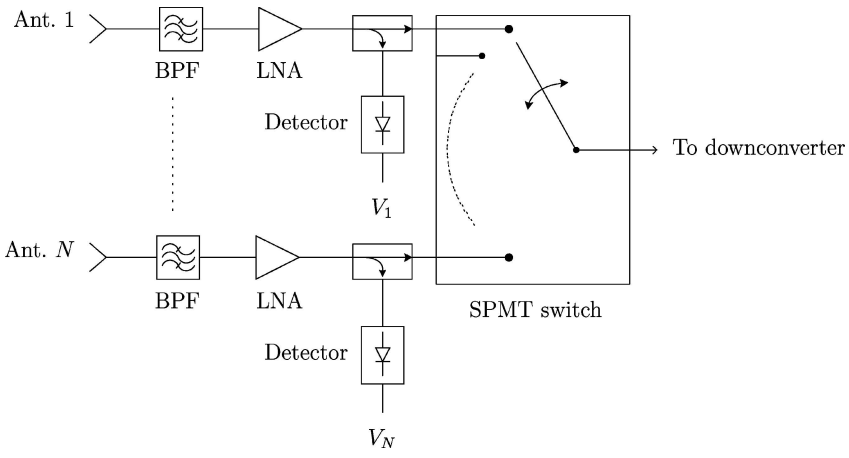

Figure 1. Proposed RF front-end architecture.

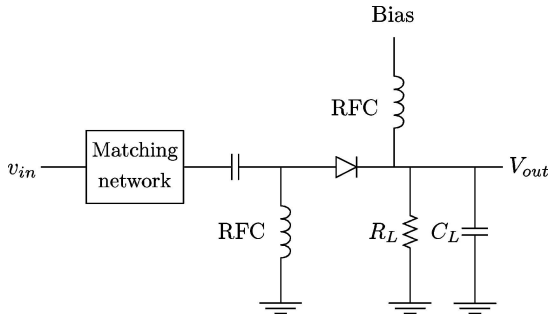

Figure 2. Envelope detector circuit example.

switching time and moderate insertion loss (less than 1 dB). See [7] for a detailed description of a PIN diode based rotary switch.

It is noteworthy that the switching transient has a duration proportional to the reciprocal of the IF bandwidth and we can expect from one to a few of the subsequent symbols to be corrupted by the transition from one branch to another. In fact, the relatively low transition time of the switch induces an almost instantaneous phase/amplitude shift which, when propagating through the remaining receiver stages expresses the impulse response of these cascaded components. Taking this into account, switching can be restriced to noninformation-bearing periods, i.e., during packet headers, tail bits and/or guard times.

2.2. The Envelope Detector

A rapid overview of the envelope detector's operation is provided here, mainly to justify analytical assumptions made later and to establish a valid SNR operation range to support design decisions.

Figure 2 details an envelope detector built around a low-cost Schottky diode. The small signal approximation of the diode current for a given voltage $v(t)$ applied at the diode is [13]:

$$I_d(v) = I_0 + vG_d + \frac{v^2}{2}G'_d \tag{1}$$

where G_d is the dynamic conductance of the diode and I_0 is the bias current.

A modulated signal $v_{\text{in}}(t)$ with carrier frequency ω_c is applied to the diode. Taking into account the fact that the acquisition chain necessary to sample the output of the envelope detector (e.g., differential amplifier, analog-to-digital converter, etc.) necessarily includes some form of low-pass filtering, terms at $\omega_c t$ and $2\omega_c t$ are rejected and the baseband current is given by:

$$I_{BB}(t) = I_0 + \frac{G'_d}{4}[I^2(t) + Q^2(t)] \tag{2}$$

$$I_{BB}(t) = I_0 + \frac{G'_d}{4}|\alpha(t)|^2. \tag{3}$$

where $I(t)$ and $Q(t)$ are the in-line and quadrature baseband components of $v_{\text{in}}(t)$.

The voltage induced by this current across the video resistance of the detector (also the output voltage of the detector) is

$$V_{BB}(t) = K + \beta|\alpha(t)|^2 \tag{4}$$

where β (the voltage sensitivity) and K (related to the bias current) are constant terms.

The small signal approximation typically remains valid for input powers up to -20 dBm, i.e., the detector is in its square-law region; beyond this point, the approximation no longer holds and a higher order model is called for. The tangential sensitivity of the detector typically is near -55 dBm for a video bandwidth of 1 MHz. Below that threshold, the output of the diode is submerged by thermal noise and no power measurement is available. In order to boost the sensitivity of the envelope detectors, LNAs are placed ahead of the envelope detector in Figure 1 (thus requiring replication across all branches). However, if the receiver is extremely sensitive, the possibility remains that the envelope detectors will be less sensitive than the receiver (depending on the LNA gain). Nonetheless, the practical impact is minimal since (1) it would only affect performance (by making incorrect branch selections) when all branches are in a deep fade, and (2) the power measurements would be unreliable in any case since they are performed on the total signal-plus-noise power.

2.3. Alternative Architecture

Another approach proposed to achieve selection diversity would be to first filter and amplify the signal from each antenna and then apply this preprocessed signal to the switch as shown in Figure 3. With this strategy, the power monitoring for the antennas is performed sequentially and must be completed during guard times since switching operations are now required. Therefore, diversity branches can be scanned in sequence and the best branch selected before information-bearing transmission is resumed. One advantage here is a further simplification of the receiver and a higher signal monitoring sensitivity. Indeed, the signal gain at the output of the downconverter and IF amplifiers is higher and the signal presented at the input of the detector is more likely to exceed its tangential sensitivity point. The downside, however, is the longer guard times required due to the additional switching.

It can be observed in Figure 3 that band filters and LNAs are replicated across all branches. Complexity could be reduced even further by using a single band filter and LNA *after* the PIN switch. This, however, decreases receiver and envelope detector sensitivities since the noise

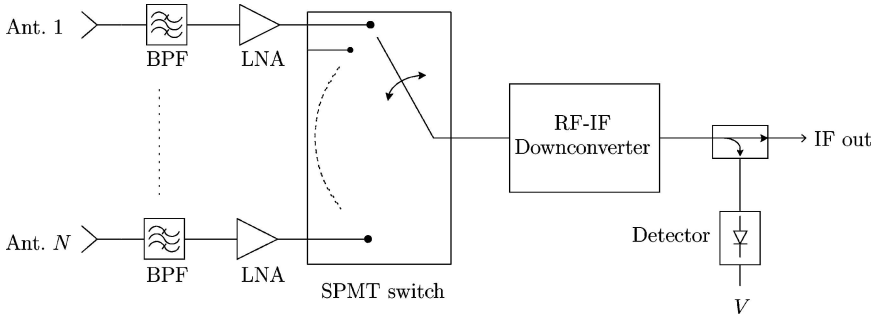

Figure 3. A variant of the proposed RF front-end architecture.

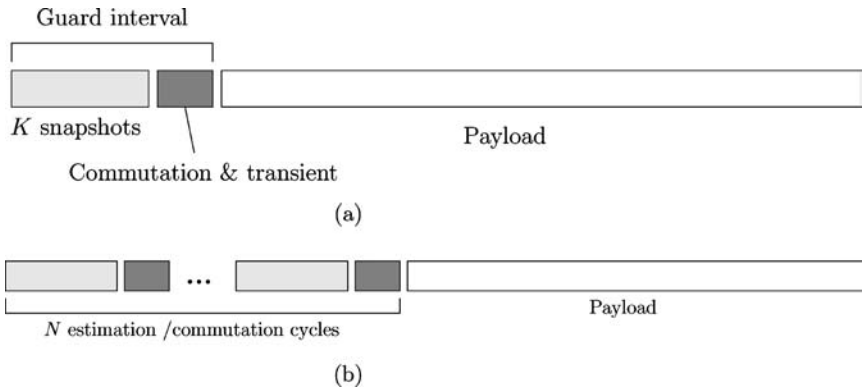

Figure 4. Packet structure with estimation and commutation intervals for (a) first SDC2 architecture and (b) second SDC2 architecture.

introduced by the PIN switch is now uphill from the LNA. In light of the extreme simplicity of the resulting receiver, this sensitivity loss may be acceptable depending on link budget and performance goals.

It should be noted that this alternative architecture has the same hardware complexity and roughly the same estimation/switching delay constraints as a switched diversity architecture [4, 5] yet yields superior performance.

2.4. Packet Structure

For such receivers to work adequately, switching activity should be restricted to guard intervals and/or training sequences to avoid losing message symbols due to switching transients. In a packet-oriented system, packets can often be assumed to be significantly smaller than the channel coherence time. Thus, at most only one power estimation/switching cycle is required per packet. This cycle requires a certain amount of time because in general it will consist of taking a number N_S of consecutive snapshots of the envelope detector's outputs, followed by a switching transient. This activity can be relegated to guard intervals (if they exist) between consecutive packets, or can be performed during training preambles/midambles/postambles since this diversity architecture does not require a training sequence.

Possible packet structures are shown in Figure 4. With the first architecture, a single estimation/switching cycle is necessary since all envelope detectors can be sampled in parallel. For the second architecture, N consecutive estimation/switching cycles are necessary in order to estimate signal power for each branch in *succession*. It follows that a longer guard interval is necessary, proportional to both N and N_S.

2.5. Incorporation in Wireless Networks

The 802.11 standard [15] and its main derivatives (802.11a [16], 802.11b [17] and 802.11g [18]) are characterized by a wide variety of physical layers in the 2.4 GHz unlicensed band (802.11, 802.11b and g), the 5 GHz unlicensed band (802.11a), or the infrared band (802.11). All these different physical layers are unified into a generic scheme known as the

Physical Layer Convergence Protocol (PLCP). In addition, a wide range of nominal data rates is supported, ranging from 1 Mb/s to 54 Mb/s. All 802.11 frames are prefixed by a PLCP preamble and a PLCP header. The PLCP preamble, composed of a synchronization sequence followed by a start frame delimiter (SFD), is of interest. Indeed, the standard explicitly states that the early portion of the sync sequence is to be used for automatic gain control *and* diversity selection, while the latter portion serves for coarse frequency offset estimation (for OFDM-based physical layers, i.e., 802.11a) and timing synchronization. The subsequent start frame delimiter is a 16-bit sequence that signals the beginning of the frame.

The PLCP preamble is always transmitted at 1 Mb/s, regardless of the effective bit rate. Furthermore, the sync sequence is relatively long: 80 bits for the frequency-hopping spread spectrum (FHSS) variant of the base 802.11 standard (with nominal bit rates of 1 and 2 Mb/s), 128 bits for the direct-sequence spread spectrum (DSSS) of the same, 128 bits or 56 bits for the 802.11b (up to 11 Mb/s nominal) and 802.11g (up to 54 Mbps nominal) variants. This provides an interval of at least 56 μs to perform the estimation/commutation cycle described above and timing synchronization. It is noteworthy that unlike other diversity architectures, the transmitted bits need not be known for antenna selection. It is only necessary to have the signal present, whatever it may contain, so that its energy can feed the envelope detectors.

For 802.11a, the picture is somewhat different. Since it is an OFDM system with different and varied estimation needs, the PLCP preamble is divided up into several specialized sections. Its sync section is composed of 10 short OFDM symbols followed by two long symbols. The early portion of the short symbol sequence (approximately seven symbols) is intended for signal detection, automatic gain control (AGC) and diversity selection. The remaining three symbols are intended for coarse frequency offset estimation and timing synchronization. The two long symbols are intended for fine frequency offset estimation and channel estimation (for equalization). The usable portion of the preamble (corresponding to the first seven short symbols) for our estimation/commutation cycle is $7 \times 0.8\,\mu\text{s} = 5.6\,\mu\text{s}$ long.

Obviously, the proposed architectures could easily be adapted to operate in 802.11 environments. Depending on the duration of switching transients and other design parameters, it may however be more difficult to apply the alternative architecture of Figure 3 to systems where the usable preamble is shorter, i.e., 802.11a. For nodes other than access points, it may also be possible to bypass the preamble altogether and rely instead on the beacon transmitted by the access point for estimation and antenna selection.

Likewise, the proposed architectures can be applied to digital cellular systems. Consider GSM for example (by far the most widespread cellular standard); each time slot comprises a known sequence near its middle (the so-called "midamble") of 26 bits for synchronization and channel estimation purposes [19]. Unlike 802.11, the full length of the midamble may be consumed by synchronization and channel estimation for equalization (a requirement in GSM) thus precluding the strategy presented above. However, it is noteworthy that handsets are assigned transmission and reception time slots which are separated in both time and frequency. They exploit the time between transmission and reception to monitor a beacon signal from their home base stations and the six strongest neighboring base stations. This, of course, serves to determine whether a handover is necessary. It seems natural to use a portion of this time – say, one time slot – also for antenna selection.

3. Performance Analysis

3.1. Ideal Selection Diversity (SDC1)

If all branches are uncorrelated and have identical average powers, the analysis of the performance of selection diversity is relatively simple and is based on *order statistics* [20]. Thus, the distribution of the output SNR is

$$f_\gamma(\gamma) = NF_x^{N-1}(\gamma) f_x(\gamma), \tag{5}$$

where $f_x(x)$ and $F_x(x)$ correspond respectively to the PDF and CDF of the branch SNR and N is the number of branches.

In Rayleigh fading with average branch SNR $\bar{\gamma}_c$, we have

$$f_\gamma(\gamma) = N \frac{e^{-\frac{\gamma}{\bar{\gamma}_c}}}{\bar{\gamma}_c} \left(1 - e^{-\frac{\gamma}{\bar{\gamma}_c}}\right). \tag{6}$$

Another, possibly simpler, approach to this problem stems from the observation [23] that the CDF of the selection diversity SNR, i.e., the probability that the array SNR γ is smaller than some value γ_o, is equal to the probability that all the branch SNRs are smaller than γ_o. Hence,

$$F_\gamma(\gamma_o) = F_x(\gamma_o)^N. \tag{7}$$

Likewise, if the branch SNRs are correlated, we have

$$F_\gamma(\gamma) = F_{x_1,x_2,\ldots,x_N}(\gamma, \ldots, \gamma), \tag{8}$$

where $F_{x_1,x_2,\ldots,x_N}(x_1, x_2, \ldots, x_N)$ is the joint CDF of the branch SNRs. However, this joint CDF does not have a known closed form for any $N \geq 2$ for all common fading distributions. While some authors have studied SDC with correlated branches [21, 22], resorting to numerical integration or infinite series is often necessary and/or the study is limited to two antennas. Therefore, derivations herein are restricted to the uncorrelated case.

3.2. Analytical Framework for SDC2

The following is a *worst-case* analysis performance-wise since it will be assumed that a single envelope detector snapshot is available to estimate the signal power ($N_S = 1$). This is done because (1) the general case of N_S snapshots is analytically difficult, (2) the case $N_S = 1$ yields an elegant and very broad result and (3) even with $N_S = 1$, decent performance can be obtained with minimal bandwidth consumption (guard times).

Let $s_n[k]$ be the useful signal on the nth branch and $\nu_n[k]$ be the noise sample on the nth branch, both quantities being sampled at the output of the matched filter at sampling instant $t = kT$ where T is the symbol period. In other words, it is assumed, without loss of generality, that the video bandwidth of the envelope detector is roughly the reciprocal of the symbol period, i.e., it acts like an approximate matched filter. It should be noted that (1) the effects of mismatched filtering are well-known and translate to a slight SNR loss; (2) the video bandwidth can be reduced to integrate the energy in more than a single symbol – this

can improve performance and/or help offset the SNR loss due to filter mismatch. However, reducing the video bandwidth does imply a longer estimation cycle. To avoid specifying the exact impulse response of the filtering applied to the envelope detector output (such filtering being at least in part implicit to the detector itself), a single parameter t_{eff} will be employed and it corresponds to the *effective* integration time, i.e., the time period over which the energy of the signal is integrated if the filtering is perfectly matched to the received pulses. Hence, $t_{\text{eff}} = T$ for standard matched filtering.

A single Schottky signal power measurement on antenna n is given by

$$a_n = |\alpha_n|^2, \quad \alpha_n = s_n + \nu_n, \tag{9}$$

where a_n is effectively the signal-plus-noise power and where the dependence on time t is implicit. Recall from Equation (4) that the output voltage V_{BB} of the detector includes a bias K and a gain β. Without loss of generality, it is assumed here that the effect of these parameters is adequately compensated, i.e., $a_n = \frac{V_{BB}-K}{\beta}$.

Given the matched filter assumption and further assuming (without loss of generality) antipodal modulation (e.g., BPSK or QPSK), we have

$$\frac{\sigma_s^2}{\sigma_\nu^2} = \frac{2E_b}{N_0}, \tag{10}$$

where E_b is the bit energy and $\frac{N_0}{2}$ is the two-sided noise power spectral density.

Alternatively, if the effective integration period t_{eff} of the envelope detector's implicit filter is longer than 1 symbol, we have

$$\frac{\sigma_s^2}{\sigma_\nu^2} = \frac{2t_{\text{eff}}E_s}{TN_0} = \frac{2\kappa E_s}{N_0}, \tag{11}$$

where $\kappa = \frac{t_{\text{eff}}}{T}$. It can be observed that the filtering has the effect of reducing the relative noise power by a factor of κ.

Therefore, the instantaneous signal-to-noise ratio of branch n is

$$\gamma_n = \frac{|s_n|^2}{\kappa\sigma_\nu^2} = \frac{|\alpha_n - \nu_n|^2}{\kappa\sigma_\nu^2}, \tag{12}$$

where $\kappa\sigma_\nu^2 = \sigma_n^2$ is the noise power. In other words, the signal-to-noise ratio at the output of the envelope detector is κ times stronger (thanks to integration over many symbols) than the signal-to-noise ratio for signal demodulation.

It follows that the signal-to-noise ratio at the output of the combiner can be expressed

$$\gamma = \sum_{n=1}^{N} \gamma_n \prod_{\substack{k=1 \\ k\neq n}}^{N} u(a_n - a_k) = \sum_{n=1}^{N} \frac{|\alpha_n - \nu_n|^2}{\kappa\sigma_\nu^2} \prod_{\substack{k=1 \\ k\neq n}}^{N} u(a_n - a_k), \tag{13}$$

where

$$u(x) = \begin{cases} 0, & x < 0, \\ 1, & x \geq 0, \end{cases} \tag{14}$$

is the Heaviside step function.

If $N = 2$, we have

$$\gamma = u(a_1 - a_2)\gamma_1 + u(a_2 - a_1)\gamma_2. \tag{15}$$

It follows that the distribution of γ conditioned on a_1 and a_2 is given by

$$f_{\gamma|a_1,a_2}(\gamma \mid a_1, a_2) = u(a_1 - a_2) f_{\gamma_1|a_1}(\gamma \mid a_1) + u(a_2 - a_1) f_{\gamma_2|a_2}(\gamma \mid a_2). \tag{16}$$

Hence, we have

$$f_\gamma(\gamma) = \int_0^\infty \int_0^\infty f_{\gamma|a_1,a_2}(\gamma \mid a_1, a_2) f_{a_1}(a_1) f_{a_2}(a_2)\, da_1 da_2. \tag{17}$$

3.3. Rayleigh Fading

Given the vector of random variables $\mathbf{x}_n^T = [\alpha_n, s_n]$, its correlation matrix is given by

$$\mathbf{R_{xx}} = \begin{bmatrix} \sigma_s^2 + \sigma_v^2 & \sigma_s^2 \\ \sigma_s^2 & \sigma_s^2 \end{bmatrix}, \tag{18}$$

where σ_s^2 is the average useful signal power.

It follows, by virtue of theorem 1.2.11 in [24] that the density of s_n conditioned on α_n is Gaussian, with a mean of $\alpha_n \frac{\sigma_s^2}{\sigma_s^2+\sigma_v^2}$ and a variance of $\sigma_v^2(\frac{\sigma_s^2}{\sigma_v^2+\sigma_s^2})$.

From (12) and given that $a_n = |\alpha_n|^2$, we have

$$f_{\gamma_n|a_n}(\gamma_n \mid a_n) = \frac{\kappa\left(\sigma_s^2 + \sigma_v^2\right)}{\sigma_s^2} e^{-\frac{a_n}{\sigma_v^2}\left(\frac{\sigma_s^2}{\sigma_s^2+\sigma_v^2}\right)} {}_0\mathrm{F}_1\left(1; \frac{\gamma_n \kappa a_n}{\sigma_v^2}\right) e^{-\kappa\gamma_n \frac{\sigma_s^2+\sigma_v^2}{\sigma_s^2}}, \tag{19}$$

which is a scaled 2-degrees-of-freedom noncentral chi-square distribution.

It is useful to observe that, in substituting (16) into (17), both terms of (16) will yield the same result after integration, provided that $f_{\gamma_1|a_1}(\gamma_1 \mid a_1) = f_{\gamma_2|a_2}(\gamma_2 \mid a_2)$ (a_1 and a_2 simply exchange roles in the two integrals). Therefore, it suffices to solve the alternate form

$$\begin{aligned} f_\gamma(\gamma) \;=\; & 2\frac{\kappa\sigma_a^2}{\sigma_s^2} \int_0^\infty \int_0^\infty u(a_1 - a_2) e^{-\frac{a_1}{\sigma_v^2}\frac{\sigma_s^2}{\sigma_a^2}} {}_0\mathrm{F}_1\left(1; \frac{\gamma\kappa a_1}{\sigma_v^2}\right) \\ & \times e^{-\gamma\kappa\frac{\sigma_a^2}{\sigma_s^2}} f_{a_1}(a_1) f_{a_2}(a_2)\, da_1 da_2, \end{aligned} \tag{20}$$

where $\sigma_a^2 = \sigma_s^2 + \sigma_v^2$ and the step function can be removed by imposing appropriate integration bounds to yield

$$f_\gamma(\gamma) \;=\; 2\frac{\kappa\sigma_a^2}{\sigma_s^2} \int_0^\infty \int_0^{a_1} e^{-\frac{a_1}{\sigma_v^2}\frac{\sigma_s^2}{\sigma_a^2}} {}_0\mathrm{F}_1\left(1; \frac{\gamma\kappa a_1}{\sigma_v^2}\right) e^{-\gamma\kappa\frac{\sigma_a^2}{\sigma_s^2}} f_{a_1}(a_1) f_{a_2}(a_2)\, da_2 da_1, \tag{21}$$

If the fading is Rayleigh with variance σ_s^2 on all branches, and the fading process is uncorrelated across the array, we have

$$f_{a_1}(x) = f_{a_2}(x) = \frac{e^{-x/\sigma_a^2}}{\sigma_a^2}. \tag{22}$$

Substituting in (21) and integrating over a_2, we get

$$f_\gamma(\gamma) = 2\frac{\kappa}{\sigma_s^2}\int_0^\infty \left(1 - e^{-\frac{a_1}{\sigma_a^2}}\right) e^{-a_1\left(\frac{1}{\sigma_a^2}+\frac{\sigma_s^2}{\sigma_v^2\sigma_a^2}\right)} e^{-\gamma\kappa\frac{\sigma_a^2}{\sigma_s^2}} {}_0\mathrm{F}_1\left(1, \frac{\gamma\kappa a_1}{\sigma_v^2}\right) da_1, \tag{23}$$

which can, in turn, be integrated term-by-term by virtue of Lemma 1.3.3 in [24] to yield

$$\begin{aligned} f_\gamma(\gamma) \;=\; & \frac{2\kappa\sigma_a^2\sigma_v^2}{\sigma_v^2\sigma_s^2+\sigma_s^4} {}_1\mathrm{F}_1\left(1;1;\gamma\frac{\kappa\sigma_a^2}{\sigma_v^2+\sigma_s^2}\right) e^{-\gamma\kappa\frac{\sigma_a^2}{\sigma_s^2}} \\ & -\frac{2\kappa\sigma_a^2\sigma_v^2}{2\sigma_v^2\sigma_s^2+\sigma_s^4} {}_1\mathrm{F}_1\left(1;1;\gamma\frac{\kappa\sigma_a^2}{2\sigma_v^2+\sigma_s^2}\right) e^{-\gamma\kappa\frac{\sigma_a^2}{\sigma_s^2}}, \end{aligned} \tag{24}$$

where ${}_1\mathrm{F}_1(a;b;x)$ is the confluent hypergeometric function. The latter has the property[1]

$${}_1\mathrm{F}_1(q;q;x) = e^x, \tag{25}$$

which, applied to (24) yields

$$f_\gamma(\gamma) = \frac{2\kappa\sigma_a^2\sigma_v^2}{\sigma_v^2\sigma_s^2+\sigma_s^4} e^{-\gamma\kappa\frac{\sigma_a^2\sigma_v^2}{\sigma_v^2\sigma_s^2+\sigma_s^4}} - \frac{2\kappa\sigma_a^2\sigma_v^2}{2\sigma_v^2\sigma_s^2+\sigma_s^4} e^{-\gamma\kappa\frac{2\sigma_a^2\sigma_v^2}{2\sigma_v^2\sigma_s^2+\sigma_s^4}}. \tag{26}$$

Likewise, it is straightforward to show (applying the same term-by-term integration technique) that the general solution for arbitrary N is

$$f_\gamma(\gamma)^{(SDC2)} = N\sum_{n=0}^{N-1}\binom{N-1}{n}(-1)^n \frac{\kappa\sigma_a^2\sigma_v^2}{(n+1)\sigma_v^2\sigma_s^2+\sigma_s^4} e^{-\gamma\kappa\frac{(n+1)\sigma_a^2\sigma_v^2}{(n+1)\sigma_v^2\sigma_s^2+\sigma_s^4}}. \tag{27}$$

The above has a form which is very close to the PDF for SDC1 if the polynomial in (6) is expanded according to the binomial theorem, i.e.,

$$f_\gamma(\gamma)^{(SDC1)} = \frac{N}{\bar{\gamma}_c}\sum_{n=0}^{N-1}\binom{N-1}{n}(-1)^n e^{-\gamma\frac{n+1}{\bar{\gamma}_c}}. \tag{28}$$

The simplicity of the forms above for $f_\gamma(\gamma)^{(SDC1)}$ and $f_\gamma(\gamma)^{(SDC2)}$ is exploited throughout the paper to obtain various performance parameters through term-by-term integration.

[1] This property is obvious when expanding ${}_1\mathrm{F}_1$ into its power series representation; however, see also [25, 7.11.1–4].

3.4. AVERAGE SNR

It is simple to show, through term-by-term integration of (28), that the average SNR at the output of a classical selection diversity combiner is

$$\bar{\gamma}^{(SDC1)} = N\bar{\gamma}_c \sum_{n=0}^{N-1} \binom{N-1}{n} \frac{(-1)^n}{(n+1)^2}. \tag{29}$$

However, it is shown in Appendix A that the above can be manipulated to reduce to the classical result [23]

$$\bar{\gamma}^{(SDC1)} = \bar{\gamma}_c \sum_{n=1}^{N} \frac{1}{n}. \tag{30}$$

Likewise, simple term-by-term integration of (27) times γ gives the average SNR of the proposed selection diversity architecture:

$$\bar{\gamma}^{(SDC2)} = N \sum_{n=0}^{N-1} \binom{N-1}{n} (-1)^n \frac{(n+1)\sigma_s^2\sigma_v^2 + \sigma_s^4}{(n+1)^2\kappa\sigma_v^2\sigma_a^2}. \tag{31}$$

Appendix B shows that the above can be reformulated as follows:

$$\bar{\gamma}^{(SDC2)} = \frac{\sigma_s^2\sigma_v^2}{\kappa\sigma_v^2\sigma_a^2} + \frac{\sigma_s^2\bar{\gamma}_c}{\sigma_a^2} \sum_{n=1}^{N} \frac{1}{n} \tag{32}$$

$$= C_1 + C_2\bar{\gamma}^{(SDC1)}, \tag{33}$$

where it can be verified, as could be expected, that C_2 is always smaller than 1.

3.5. BIT ERROR PROBABILITY

It is noteworthy that the general result (27) for the density of the output SNR can be expressed as follows:

$$f_\gamma(\gamma) = N \sum_{n=0}^{N-1} \binom{N-1}{n} \frac{(-1)^n}{1+n} g_{\gamma_0}\left(\gamma, \frac{(n+1)\sigma_v^2\sigma_s^2 + \sigma_s^4}{(n+1)\kappa\sigma_a^2\sigma_v^2}\right), \tag{34}$$

where

$$g_{\gamma_0}(\gamma, \bar{\gamma}_c) = \frac{e^{-\frac{\gamma_0}{\bar{\gamma}_c}}}{\bar{\gamma}_c}, \tag{35}$$

which is a 2 degrees-of-freedom scaled central chi-square distribution and it corresponds to the ideal SNR at the output of a single branch receiver operating in a Rayleigh-fading environment with an average SNR of $\bar{\gamma}_c$.

It follows that the output SNR distribution (34) can be assimilated to a linear mixture of the output SNRs of $N-1$ ideal single-branch receivers. Likewise, the bit error probability

(BEP) for any modulation scheme is the same linear mixture of bit error probabilities for the corresponding ideal single branch receivers, i.e.,

$$P_2^{(SDC2)} = N \sum_{n=0}^{N-1} \binom{N-1}{n} \frac{(-1)^n}{1+n} P_2\left(\frac{(n+1)\sigma_v^2\sigma_s^2 + \sigma_s^4}{(n+1)\kappa\sigma_a^2\sigma_v^2}\right), \tag{36}$$

where $P_2(\bar{\gamma}_c)$ is the corresponding BEP for a single-branch receiver averaged over Rayleigh fading with a mean SNR of $\bar{\gamma}_c$.

This is convenient because bit error probabilities P_2 in Rayleigh fading are well-known for virtually any modulation scheme and can be directly substituted in (36). For example, it is known that [26]

$$P_2^{(DPSK)}(\bar{\gamma}_c) = \frac{1}{2}\frac{1}{1+\bar{\gamma}_c}. \tag{37}$$

The above, when substituted in (36), yields

$$P_2^{(SDC2,DPSK)} = \frac{N}{2} \sum_{n=0}^{N-1} \binom{N-1}{n} \frac{(-1)^n}{1+n} \frac{\kappa(n+1)\sigma_a^2\sigma_v^2}{(n+1)\sigma_v^2\left(\kappa\sigma_a^2 + \sigma_s^2\right) + \sigma_s^4}. \tag{38}$$

An alternate form for (38) is given later which is more convenient for numerical evaluation (see Section 4 and Appendix D).

Similar expressions can be found for other modulation schemes using the same approach. Also, it is easy to show (see Appendix C) that the BEP for classical selection diversity combining is

$$P_2^{(SDC1)} = N \sum_{n=0}^{N-1} \binom{N-1}{n} \frac{(-1)^n}{n+1} P_2\left(\frac{\bar{\gamma}_c}{n+1}\right), \tag{39}$$

from which expressions can be derived for any modulation scheme as was done for SDC2.

3.6. Outage Probability

It is well-known that the average BEP can in some circumstances be a misleading performance parameter, since the average picture provides no indication as to the severity and frequency of occurrence of performance drops. For this reason, it is of interest to study outage probability which is defined simply as the probability that performance will drop below a predefined threshold (the outage point).

If the outage point is situated at $\gamma = \gamma_o$, we have

$$P_{\text{out}}(\gamma_o) = P(\gamma < \gamma_o) = F_\gamma(\gamma_o) = \int_0^{\gamma_o} f_\gamma(\gamma)\, d\gamma. \tag{40}$$

Since, in a white noise environment, the relation between the BEP and P_{out} is monotonic, the above definition remains valid if the outage point is defined in terms of the average BEP. It suffices to find a γ_o such that

$$P_{e_o} = P_e(\gamma_o), \tag{41}$$

where P_{e_o} is the outage point defined in terms of the average BEP and $P_e(\gamma)$ is the BEP as a function of instantaneous SNR γ.

In Rayleigh-fading, the outage probability for SDC2 can be obtained by substituting (27) in (40) and performing term-by-term integration.

Thus, we obtain

$$P_{\text{out}}(\gamma_o) = P(\gamma < \gamma_o) = N \sum_{n=0}^{N-1} \binom{N-1}{n} \frac{(-1)^n}{n+1} \left(1 - e^{-\gamma_o \kappa \frac{\sigma_a^2 \sigma_v^2 (n+1)}{(n+1)\sigma_v^2 \sigma_s^2 + \sigma_s^4}}\right). \tag{42}$$

For ideal selection diversity, the outage probability is given by (7).

4. Performance as a Function of Dwell Time

We now examine the impact of relaxing the coherence time constraint. In other words, it is assumed that the packet structure detailed in Section 2.4 is maintained, but that packet lengths are not necessarily shorter than the channel coherence time. This implies that a given branch selection has to be maintained beyond the point in time where it is still an optimal choice.

The degradation in performance due to dwell time was studied in [1, 2], but it is presented here in conjunction with imperfect SNR estimation and the approach therefore differs.

We wish to find the distribution of the output SNR γ as a function of the delay τ (dwell time) since the last estimation/commutation cycle. At $\tau = 0$, the PDF is given by (27). When τ is sufficiently large to ensure complete channel decorrelation with respect to $\tau = 0$, the system performance reduces to that of a single-antenna receiver, and we have

$$f_\gamma(\gamma) = \frac{e^{-\frac{\gamma}{\bar{\gamma}_c}}}{\bar{\gamma}_c}, \tag{43}$$

where the average channel SNR $\bar{\gamma}_c = \frac{\sigma_s^2}{\kappa \sigma_v^2}$.

Without loss of generality, it is assumed that the channel autocorrelation function is based on the Jakes fading spectrum [28] (isotropic scattering assumption), i.e.,

$$R(\tau) = R_{xx}(\tau) = R_{yy}(\tau) = \mathrm{J}_0\left(\frac{2\pi v \tau}{\lambda}\right), \tag{44}$$

where x and y are the orthogonal components of the complex channel gain and v is the speed of the receiver with respect to the transmitter.

Furthermore, the PDF (27) is actually a sum of exponential subdistributions. These can be individually considered as the SNR PDF associated with a complex Gaussian channel gain. Observing one such channel gain over time, its variance will slowly reduce to $\bar{\gamma}_c$ as channel decorrelation is achieved.

It follows that the complex gaussian variance as a function of τ for subdistribution n is given by

$$\sigma^2(\tau) = R^2(\tau) \frac{(n+1)\sigma_v^2 \sigma_s^2 + \sigma_s^4}{(n+1)\kappa \sigma_a^2 \sigma_v^2} + (1 - R^2(\tau)) \frac{\sigma_s^2}{\kappa \sigma_v^2}. \tag{45}$$

Hence, we have

$$f_{\gamma(\tau)}(\gamma(\tau)) = N\sum_{n=0}^{N-1}\binom{N-1}{n}\frac{(-1)^n\kappa\sigma_a^2\sigma_v^2}{(n+1)\sigma_v^2\sigma_s^2+(1-R^2(\tau))n\sigma_s^4+\sigma_s^4} \times e^{-\gamma(\tau)\kappa\frac{(n+1)\kappa\sigma_a^2\sigma_v^2}{(n+1)\sigma_v^2\sigma_s^2+(1-R^2(\tau))n\sigma_s^4+\sigma_s^4}}, \tag{46}$$

and it can be verified that the above reduces to (27) when $R(\tau) = 1$, and reduces to (43) when $R(\tau) = 0$. The latter is true since

$$N\sum_{n=0}^{N-1}\binom{N-1}{n}\frac{(-1)^n}{n+1} = \sum_{n=0}^{N-1}\binom{N}{n+1}(-1)^n = \sum_{k=1}^{N}\binom{N}{k}(-1)^{k-1}$$
$$= -\sum_{k=0}^{N}\binom{N}{k}(-1)^k + 1 = (1-1)^N + 1 = 1.$$

It follows that (36) can be generalized to become

$$P_2^{(SDC2)}(\tau) = N\sum_{n=0}^{N-1}\binom{N-1}{n}\frac{(-1)^n}{1+n}P_2\left(\frac{(n+1)\sigma_v^2\sigma_s^2+(1-R^2(\tau))n\sigma_s^4+\sigma_s^4}{(n+1)\kappa\sigma_a^2\sigma_v^2}\right). \tag{47}$$

Like many other results in this paper, the above is in the form of an alternate sum. Such forms are notoriously difficult to evaluate numerically and Appendix D shows that (47) can be rewritten as follows in the DPSK case:

$$P_2^{(SDC2,DPSK)}(\tau) = \frac{N!\kappa\sigma_a^2}{2\left(\kappa\sigma_a^2+\sigma_s^2\right)}\frac{\Gamma\left(\frac{(\kappa\sigma_a^2+\sigma_s^2)+\sigma_s^4/\sigma_v^2}{\kappa\sigma_a^2+\sigma_s^2+(1-R^2(\tau))\sigma_s^4/\sigma_v^2}+1\right)}{\Gamma\left(\frac{(\kappa\sigma_a^2+\sigma_s^2)+\sigma_s^4/\sigma_v^2}{\kappa\sigma_a^2+\sigma_s^2+2(1-R^2(\tau))\sigma_s^4/\sigma_v^2}+N\right)}. \tag{48}$$

Finally, the average bit error rate for a packet is given by

$$\bar{P}_2 = \int_0^{\tau_p} P_2(\tau)\,d\tau, \tag{49}$$

where τ_p is the packet duration.

5. Numerical Results

Figure 5 compares the outage probability of SDC1 and SDC2 for 2, 4, 8 and 25 antenna elements. The outage point is defined as the probability that the instantaneous BEP is smaller than 10^{-3} when coherent QPSK is employed.

Figure 6 shows the BEP as a function of the same set of parameters for DPSK. It can be observed that the gap between SDC1 and SDC2 with $\kappa = 1$ is slightly larger in general for DPSK than for coherent QPSK.

Figure 7 shows the average BEP performance $\bar{P}_2$ as a function of the normalized delay, i.e., delay τ times the fading bandwidth B_f for 2, 4, 8 and 25 antennas, branch input SNRs

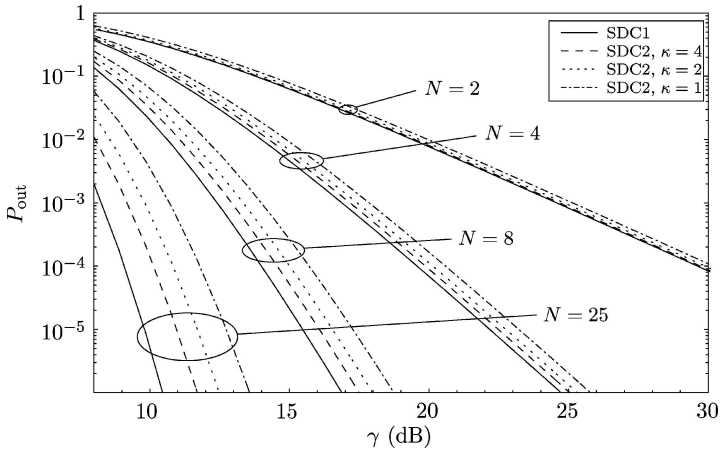

Figure 5. Outage probability with the outage point defined by the probability $P(P_e < 10^{-3})$ when coherent QPSK is employed.

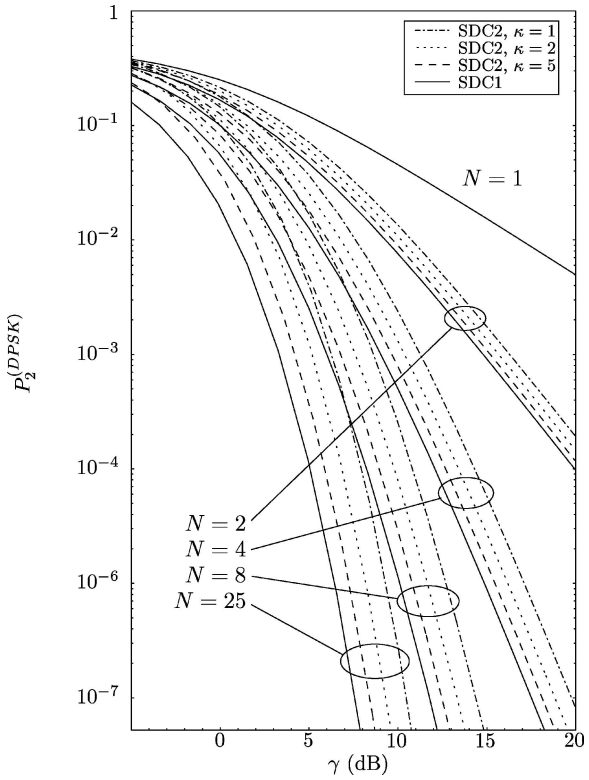

Figure 6. Bit error probability for various array sizes and values of κ when DPSK is employed.

ranging from 0 to 40 dBs, and $\kappa = 1, 2, 5$ and ∞ (i.e., SDC1). For the Jakes fading spectrum, $B_f = \frac{v}{\lambda}$. Results are consistent with those reported in [1, 2] and show an increased sensitivity to the dwell time as the number of antennas augments. The impact of different magnitudes of estimation error, however, does not affect the said sensitivity.

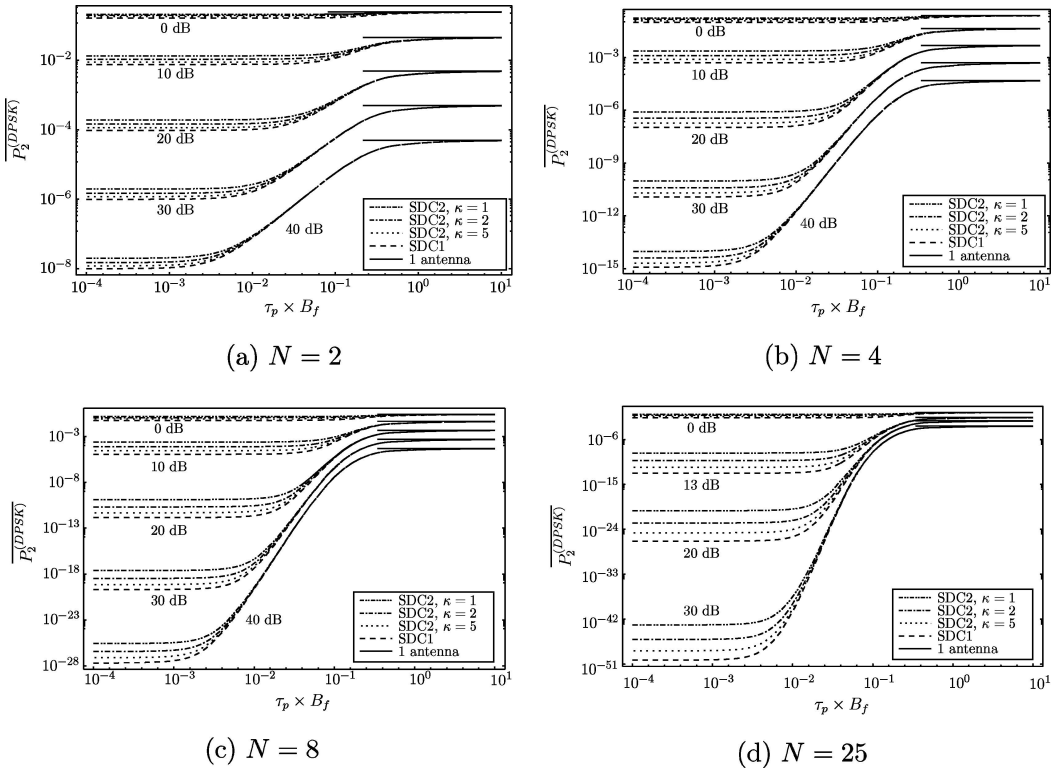

Figure 7. Average BEP performance as a function of normalized packet duration (duration τ_p times the fading bandwidth B_f) for $N = 2$, 4, 8 and 25 antennas for various branch SNRs.

6. Conclusion

A simple architecture for a selection diversity combiner was presented. Based on switching means and inexpensive Schottky-diode based envelope detectors, it requires only a single complete downconversion/reception chain and thus minimizes component replication. An analytical framework was provided characterizing the performance of such an architecture, where the power measurements are performed on the overall signal-plus-noise envelope. A discussion was provided illustrating how such a scheme could be applied to existing wireless networks including 802.11 wireless LANs and GSM cellular networks. Numerical results have shown that performance is very near to the ideal, classical selection diversity scheme when the SNR is sufficiently high. It can in fact be made arbitrarily close to the ideal selection diversity performance by altering the envelope detector's bandwidth, at the possible cost of a longer estimation interval.

Closed-form expressions for the average bit error probability (for DPSK), the outage probability, and the average SNR have been derived for SDC2 in Rayleigh fading, in addition to the PDF of the output SNR γ. The parameter κ corresponds to the temporal length of the envelope detector filtering and thus indicates the amount of effective estimation noise.

It is of interest that the average SNR, average BEP and outage probability results can be expressed as finite sums of the same parameter for single-branch receivers. Thus, well-known classical results for any common modulation scheme can be exploited, making such results very broad, provided that uncorrelated Rayleigh fading is assumed.

The performance penalty versus ideal SDC is less than 1 dB in terms of average BEP with DPSK modulation and $\kappa = 5$. As could be expected, the performance gap grows with the number of antennas. It also seems to grow faster for outage probability than for average BEP. Finally, analysis of the combined impact of prolonged dwell time and estimation error, as well as associated numerical results, corroborates the results of [1, 2] and shows clearly that the two effects are largely independent.

Appendix A

Given

$$\bar{\gamma}^{(SDC1)} = N\bar{\gamma}_c \sum_{n=0}^{N-1} \binom{N-1}{n} \frac{(-1)^n}{(n+1)^2} = \bar{\gamma}_c \sum_{n=0}^{N-1} \binom{N}{n+1} \frac{(-1)^n}{(n+1)}, \tag{A1}$$

we can apply the following Gamma function identity

$$\frac{\Gamma(z-k)}{\Gamma(z)} = \frac{(-1)^k \Gamma(1-z)}{\Gamma(1-z+k)}, \tag{A2}$$

to obtain

$$\bar{\gamma}^{(SDC1)} = -\bar{\gamma}_c \sum_{n=0}^{N-1} \frac{\Gamma(n+1-N)}{\Gamma(-N)(n+1)!} \frac{1}{n+1}, \tag{A3}$$

which, if the factor $1/(n+1)$ is written in terms of Gamma functions and the numerator and denominator are both multiplied by $n! = \Gamma(n+1)$, becomes

$$\bar{\gamma}^{(SDC1)} = -\bar{\gamma}_c \sum_{n=0}^{N-1} \frac{\Gamma(n+1-N)\Gamma(n+1)^2}{\Gamma(-N)\Gamma(n+2)^2 n!}. \tag{A4}$$

According to the series definition of hypergeometric functions, the above is expressible as

$$\bar{\gamma}^{(SDC1)} = \bar{\gamma}_c N {}_3\mathrm{F}_2(1-N, 1, 1; 2, 2; 1), \tag{A5}$$

which, by virtue of identity [25, 7.4.4-49] is equivalent to

$$\bar{\gamma}^{(SDC1)} = \bar{\gamma}_c N \frac{\Gamma(2)\Gamma(N)}{\Gamma(1+N)} \left(\psi(1+N) - \psi(1)\right), \tag{A6}$$

where $\psi(z)$ is the *psi function* (the logarithmic derivative of the Gamma function) and corresponds to the series [27, p. 496]

$$\psi(z) = -C + \sum_{n=0}^{\infty} \left(\frac{1}{n+1} - \frac{1}{z+n} \right), \tag{A7}$$

where C is a constant (the Euler–Mascheroni constant).

In (A6), we observe that

$$N \frac{\Gamma(2)\Gamma(N)}{\Gamma(1+N)} = N \frac{1}{N} = 1. \tag{A8}$$

Furthermore, we have

$$\begin{aligned} \left(\psi(1+N) - \psi(1)\right) &= -C + \sum_{n=0}^{\infty} \left(\frac{1}{n+1} - \frac{1}{1+N+n} \right) + C - \sum_{n=0}^{\infty} \left(\frac{1}{n+1} - \frac{1}{1+n} \right) \\ &= \sum_{n=0}^{\infty} \left(\frac{1}{n+1} - \frac{1}{1+N+n} \right) \\ &= \sum_{n'=1}^{N} \frac{1}{n'} \end{aligned} \tag{A9}$$

which leads to the result published in 1954 by Brennan [23, Appendix VI]

$$\bar{\gamma}^{(SDC1)} = \bar{\gamma}_c \sum_{n=1}^{N} \frac{1}{n}. \tag{A10}$$

Brennan's derivation is based on attacking directly the integral for the average SNR (without prior expansion of the polynomial), through a substitution and subsequent expansion in infinite series of part of the integrand. Our approach (term-by-term integration, representation of the result as a hypergeometric series, and subsequent simplification) has the virtue of being applicable also to SDC2 and the BER of DPSK for both SDC1 and SDC2 (see Appendices B and D).

Appendix B

Separating (31) into two sums, we get

$$\bar{\gamma}^{(SDC2)} = \frac{\sigma_s^2\sigma_v^2}{\kappa\sigma_v^2\sigma_a^2} T_1 + \frac{\sigma_s^4}{\kappa\sigma_v^2\sigma_a^2} T_2, \tag{B11}$$

where

$$T_1 = N \sum_{n=0}^{N-1} \binom{N}{n} \frac{(-1)^n}{(n+1)}, \tag{B12}$$

and

$$T_2 = N \sum_{n=0}^{N-1} \binom{N}{n} \frac{(-1)^n}{(n+1)^2}. \tag{B13}$$

Since T_2 has the same form as the sum treated in Appendix A, we can apply the result therein to get

$$T_2 = \sum_{n=1}^{N} \frac{1}{n}. \tag{B14}$$

Applying the identity (A2) to T_1, the following alternate representation is obtained:

$$T_1 = N \sum_{n=0}^{N-1} \frac{\Gamma(1-N+n)\Gamma(n+1)}{\Gamma(1-N)n!\Gamma(n+2)}. \tag{B15}$$

This sum now has a structure which matches that of the Gauss hypergeometric function and can be written

$$T_1 = N\,{}_2\mathrm{F}_1(1-N, 1; 2; 1), \tag{B16}$$

to which the following identity can be applied [27, p. 508]:

$${}_2\mathrm{F}_1(a, b, c; 1) = \frac{\Gamma(c-a-b)\Gamma(c)}{\Gamma(c-a)\Gamma(c-b)}, \qquad \text{iff } c-a-b > 0, \tag{B17}$$

to yield

$$T_1 = N \frac{\Gamma(N)}{\Gamma(1+N)} = 1. \tag{B18}$$

Therefore, substituting (B18) and (B14) into (B11), we finally obtain

$$\bar{\gamma}^{(SDC2)} = \frac{\sigma_s^2\sigma_v^2}{\kappa\sigma_v^2\sigma_a^2} + \frac{\sigma_s^4}{\kappa\sigma_v^2\sigma_a^2} \sum_{n=1}^{N} \frac{1}{n} = \frac{\sigma_s^2\sigma_v^2}{\kappa\sigma_v^2\sigma_a^2} + \frac{\bar{\gamma}_c\sigma_s^2}{\sigma_a^2} \sum_{n=1}^{N} \frac{1}{n}. \tag{B19}$$

Appendix C

The bit error probability in Rayleigh fading of classical selection diversity is given by

$$P_2^{(SDC1)} = \int_0^\infty P_e(\gamma) f_\gamma(\gamma)\, d\gamma, \tag{C20}$$

where $P_e(\gamma)$ is the bit error probability expression for the modulation scheme of interest and $f_\gamma(\gamma)$ has the form of Equation (5).

Substituting (28) in (C20), we obtain

$$P_2^{(SDC1)} = N \sum_{n=0}^{N-1} \binom{N-1}{n} \frac{(-1)^n}{n+1} \int_0^\infty P_e(\gamma) g_{\gamma_0}\left(\gamma, \frac{\bar{\gamma}_c}{n+1}\right) d\gamma, \tag{C21}$$

where $g_{\gamma_0}(\gamma, \frac{\bar{\gamma}_c}{n+1})$ is as defined in (35) and is the density of the SNR at the output of a single branch receiver operating in Rayleigh fading with an average SNR of $\frac{\bar{\gamma}_c}{n+1}$. It follows that the integral corresponds to the bit error probability (with the modulation scheme of interest) of a single branch receiver averaged over Rayleigh fading, thus leading to

$$P_2^{(SDC1)} = N \sum_{n=0}^{N-1} \binom{N-1}{n} \frac{(-1)^n}{n+1} P_2\left(\frac{\bar{\gamma}_c}{n+1}\right), \tag{C22}$$

which holds for any common type of modulation.

However, given the numerical evaluation problems sometimes associated with alternate sums, is may be desirable to derive from the above a different formulation whenever possible.

For example, for DPSK we have

$$P_2^{(SDC1,DPSK)} = \sum_{n=1}^{N-1} \binom{N-1}{n+1} \frac{(-1)^n}{n+1+\bar{\gamma}_c}, \tag{C23}$$

which, according to a development similar to that of Appendix A, reduces to the well-known result

$$P_2^{(SDC1,DPSK)} = \frac{N}{2} \mathrm{B}(1+\bar{\gamma}_c, N), \tag{C24}$$

where $B(a,b) = \frac{\Gamma(a)\Gamma(b)}{\Gamma(a+b)}$ is the Beta function.

Appendix D

From (47) and (37) and through straightforward algebraic manipulations, it can be shown that (38) can be written in the following form:

$$P_2^{(SDC2,DPSK)}(\tau) = \frac{N}{2} \sum_{n=0}^{N-1} \binom{N-1}{n} \frac{(-1)^n}{An+B}, \tag{D25}$$

where

$$A = \frac{2\kappa\sigma_a^2 + 2\sigma_s^2 + 2(1-R^2(\tau))\frac{\sigma_s^4}{\sigma_v^2}}{\kappa\sigma_a^2} \tag{D26}$$

$$B = \frac{2\kappa\sigma_a^2 + 2\sigma_s^2}{\kappa\sigma_a^2} + \frac{2\sigma_s^4}{\kappa\sigma_a^2\sigma_v^2}. \tag{D27}$$

Applying the gamma function identity (A2), we get

$$P_2^{(SDC2,DPSK)}(\tau) = \frac{N}{2A} \sum_{n=0}^{N-1} \frac{\Gamma(-N+n)}{\Gamma(-N)n!} \frac{1}{n+\frac{B}{A}}, \tag{D28}$$

where the factor $\frac{1}{n+\frac{B}{A}}$ can be expressed in terms of gamma functions by virtue of $\Gamma(z+1) = z\Gamma(z)$ to yield

$$P_2^{(SDC2,DPSK)}(\tau) = \frac{N}{2A} \sum_{n=0}^{N-1} \frac{\Gamma(1-N+n)}{\Gamma(1-N)n!} \frac{\Gamma\left(n+\frac{B}{A}\right)}{\Gamma\left(n+\frac{B}{A}+1\right)}. \tag{D29}$$

The summation is now in a form which corresponds exactly with the Gauss hypergeometric function [25] and reduces to

$$P_2^{(SDC2,DPSK)}(\tau) = \frac{N}{2A}\,{}_2\mathrm{F}_1\left(-N+1, \frac{B}{A}, \frac{B}{A}+1; 1\right)\frac{A}{B}. \tag{D30}$$

Noting that the A's cancel out and given that ${}_2\mathrm{F}_1(a, b, c; x)$ with $x = 1$ reduces to a ratio of Gamma functions by virtue of (B17), it is finally found that

$$P_2^{(SDC2,DPSK)}(\tau) = \frac{N}{2B}\,\frac{\Gamma\left(\frac{B}{A}+1\right)\Gamma(N)}{\Gamma\left(\frac{B}{A}+N\right)}. \tag{D31}$$

References

1. J.A. Ritcey and M. Azizoğlu, "Impact of switching constraints on selection diversity performance," in *Proceedings 32nd Asilomar Signals, Systems and Computer Conference*, Pacific Grove, California, Vol. 1, pp. 795–799, November 1998.
2. J.H. Barnard and C.K. Pauw, "Probability of error for selection diversity as a function of dwell time," *IEEE Trans. Commun.*, Vol. 37, No. 8, pp. 800–803, August 1989.
3. G.D. Durgin, *Space-Time Wireless Channels*. Upper Saddle River, Prentice-Hall, pp. 213–214, 2003.
4. A.A. Abu-Dayya and N.C. Beaulieu, "Analysis of switched-diversity systems on generalized-fading channels," *IEEE Trans. Commun.*, Vol. 42, No. 11, November 1994.
5. Y.-C. Ko, M.-S. Alouini and M.K. Simon, "Analysis and optimization of switched diversity systems," *IEEE Trans. Vehic. Tech.*, Vol. 49, No. 5, September 2000.
6. E.A. Neasmith and N.C. Beaulieu, "New results on selection diversity," *IEEE Trans. Commun.*, Vol. 46, No. 5, pp. 695–704, May 1998.
7. Q. Wang, M. Lecours and C. Vergnolle, "Criteria for wide-band radial switch design," *IEEE Trans. Microwave Theory and Techniques*, Vol. 49, No. 1, January 2001.
8. Y.G. Kim and S.W. Kim, "Optimum selection diversity for BPSK signals in Rayleigh fading channels," *IEEE Trans. Commun.*, Vol. 49, No. 10, pp. 1715–1718, October 2001.
9. G.F. Montgomery, "Message error in diversity frequency-shift reception," *Proc. IRE*, Vol. 45, pp. 1184–1187, July 1954.
10. G.-T. Chyi, J.G. Proakis, and C.M. Keller, "On the symbol error probability of maximum-selection diversity reception schemes over Rayleigh fading channels," *IEEE Trans. Comm.*, Vol. 37, pp. 79–83, Jan. 1989.
11. M.-S. Alouini and M.K. Simon, "Postdetection switched combining – A simple diversity scheme with improved BER performance," *IEEE Trans. Comm.*, Vol. 51, No. 9, pp. 1591–1602, September 2003.
12. M.K. Simon and M.-S. Alouini, "Probability of error for noncoherent M-ary orthogonal FSK with postdetection switched combining," *IEEE Trans. Comm.*, Vol. 51, No. 9, pp. 1456–1462, September 2003.
13. David M. Pozar, *Microwave engineering*, 2nd ed, J. Wiley & Sons, New York, 1998.
14. Agilent Technologies Application Note 923, *Schottky barrier diode video detectors*.
15. —, *ANSI/IEEE Std 802.11, 1999 Ed.: Part 11: Wireless LAN medium access control (MAC) and physical layer (PHY) specifications*. IEEE, Piscataway, NJ, U.S.A., 1999.
16. —, *IEEE Std 802.11a-1999 (Supplement to IEEE Std 802. 11-1999): Part 11: Wireless LAN medium access control (MAC) and physical layer (PHY) specifications – High-speed physical layer in 5 GHz band*, IEEE, Piscataway, NJ, U.S.A., 1999.
17. —, *IEEE Std 802.11b-1999 (Supplement to IEEE Std 802. 11-1999): Part 11: Wireless LAN medium access control (MAC) and physical layer (PHY) specifications – Higher-speed physical layer extension in the 2.4 GHz band*, IEEE, Piscataway, NJ, U.S.A., 1999.
18. —, *IEEE Std 802.11g-2003 (Amendment to IEEE Std 802.11-1999): Part 11: Wireless LAN medium access control (MAC) and physical layer (PHY) specifications – Amendment 4: further higher data rate extension in the 2.4 GHz band*, IEEE, Piscataway, NJ, U.S.A., 2003.
19. V.K. Garg and J.E. Wilkes, *Principles and applications of GSM*, Prentice-Hall, Upper Saddle River, NJ, U.S.A., 1999.
20. A. Papoulis and S.U. Pillai, *Probability, random variables and stochastic processes, 4th ed.*, McGraw-Hill, New York, 2002.

21. O.C. Ugweje and V.A. Aalo, "Performance of selection diversity system in correlated Nakagami fading," in *Proc. 47th IEEE Vehic. Tech. Conf. (VTC'97)*, Vol. 3, pp. 1488–1492, May 1997.
22. L. Fang and G. Bi, "Performance of selection diversity reception in correlated Rayleigh fading channels," *Electron. Letters*, Vol. 34, No. 11, pp. 1071–1072, May 1998.
23. D.G. Brennan, "Linear diversity combining techniques," *Proc. IRE*, Vol. 47, pp. 1075–1102, June 1959.
24. R.J. Muirhead, *Aspects of Multivariate Statistical Theory*. New York: J. Wiley & Sons, 1982.
25. A.P. Prudnikov, Y.A. Brychkov and O.I. Marichev, *Integrals and Series vol. 3: More Special Functions*. Gordon and Breach Science Publishers, Amsterdam, 1990.
26. J. Proakis, *Digital Communications*. McGraw-Hill, New York, 1995.
27. D. Zwillinger, ed., *Standard Mathematical Tables and Formulae, 30th ed* . CRC Press, Boca Raton, 1996.
28. W.C. Jakes, *Microwave mobile communications*. J. Wiley & Sons, New York, 1974.

Sebastien Roy received the B. Sc. A. and M. Sc. degrees in electrical engineering from l'Université Laval, Québec, Canada, in 1991 and 1993, respectively, and the Ph.D. degree from Carleton University, Ottawa, Canada, in 2000. He is currently an Assistant Professor at the Department of Electrical and Computer Engineering, Université Laval, where he is pursuing research in the system-level and implementation aspects of signal processing for communications as well as space-time processing and space-time coding. From 2000 to 2002, he was a Natural Sciences and Engineering Research Council of Canada Postdoctoral Fellow at l'Université Laval. He has been active in industrial consulting and was involved in the organization of an international conference. Prof. Roy received the Post-Graduate Research Excellence Award from the Canadian Institute of Telecommunications Research in 2000.

Jean-Sébastien Néron received the B.Sc. degree in electrical engineering from École de technologie supérieure, Montréal, Canada in 2000 and the M.Sc. degree in electrical engineering from Laval University, Québec, Canada in 2005. He is currently working towards the Ph.D. degree on the design and realization of a wideband millimeter-wave smart antenna. He acquired industrial experience in various R&D departments especially on RF Modems, RF measurements and characterization, and embedded systems design. His research interests include planar antennas, microwave circuits, and channel characterization at millimetre-wave frequencies.